Review

Optical small animal imaging in the drug discovery process

S. Dufort [a,b,c,1], L. Sancey [a,b,1], C. Wenk [a,b], V. Josserand [a,b], J.L. Coll [a,b,*]

[a] CRI-INSERM U823, Cibles diagnostiques ou thérapeutiques et vectorisation de drogues dans les cellules tumorales, Institut Albert Bonniot, BP 170, 38 042 Grenoble cedex 9, France
[b] Université Joseph Fourier, BP 53, 38 041 Grenoble cedex 9, France
[c] UF Cancérologie Biologique et Biothérapie, pôle de biologie et pathologie, CHU de Grenoble, BP 217, 38 043 Grenoble cedex 9, France

ARTICLE INFO

ABSTRACT

Molecular imaging of tumors in preclinical models is of the utmost importance for developing innovative cancer treatments. This field is moving extremely rapidly, with recent advances in optical imaging technologies and sophisticated molecular probes for *in vivo* imaging. The aim of this review is to provide a succinct overview of the imaging modalities available for rodents and with focus on describing optical probes for cancer imaging.

Contents

1. Introduction

Molecular imaging can be used as a non-invasive means to evaluate pathophysiological processes, such as cancer, in rodents. Indeed, these techniques provide real-time information for early diagnosis, allow longitudinal follow-up of tumor development, and facilitate studies of therapeutic activity and antitumor efficacy of new anti-cancer drugs. Because drug development is an expensive and complicated process with an extremely slim chance of success for any given molecule, molecular imaging can play an important role in drug discovery in the laboratory, during the translation phase from *in vitro* assays to preclinical systems, and eventually in evaluating the biodistribution, pharmacokinetics and biological activity of potentially therapeutics molecules [1].

These applications necessitate the generation of suitable imaging devices and imaging probes. This review presents the most commonly used methods for small animal imaging. We will focus mainly on optical imaging techniques and probes that are actively being developed for their sensitivity, inherent biological safely, and relative ease of use (see Table 1). In addition, we will present the translation of novel optical devices, methods and techniques into the clinic, which are areas of increased interest.

2. Commonly used small animal imaging technologies

2.1. X-ray computed tomography (CT)

CT is very commonly used on human patients, but until recently its application in rodents has been limited by its spatial resolution. X-rays are absorbed to varying degrees by different biological tissues. Recently, micro-CT devices have been developed to image rodents with a spatial resolution ranging from 10 to 100 μm [2]. Micro-CT is a powerful and cost-effective method for imaging soft-tissue structures, skeletal abnormalities and tumors. Micro-CT systems provide excellent sensitivity for skeletal tissue (Table 1).

2.2. Magnetic resonance imaging (MRI)

MRI is another standard method of clinical imaging, and recent improvements and adaptations have expanded its use to specialized animal facilities. ^{1}H-MRI is based on the fact that when a sample lying within a magnetic field is subjected to a radio-frequency pulse its protons absorb energy and generate a detectable signal during the relaxation phase. The strength of the signal is a function of the number of protons. The relaxation process can be described by two fundamental rate constants: T1 (longitudinal relaxation) and T2 (transverse relaxation) [3]. The sensitivity of this method is low (mM concentrations) but its spatial resolution is extremely good (μm). MRI is very useful for detecting tumors and measuring morphologic parameters. Because there is no damaging radiation, multiple imaging sessions can be performed safely, allowing longitudinal follow-up of tumor growth. Finally, contrast agents influencing either the T1 or T2 relaxation time constants are being developed to allow functional imaging [4–7].

2.3. PET and SPECT

Positron emission tomography (PET) requires the use of radioactive isotopes that emit positrons, such as ^{18}F, ^{15}O, ^{13}N, and ^{11}C [8], while SPECT (single photon emission computed tomography) uses tracers that emit gamma ray or high-energy X-ray photons, such as ^{123}I, ^{125}I, and ^{99}mTc. Positrons move a short distance through tissues, losing energy as they collide with other molecules, and eventually combine with electrons ("annihilation"), producing two high-energy gamma rays or photons traveling outward and in opposite directions. In SPECT, a single photon per event is directly emitted, and this photon interacts with electrons and nuclei of nearby atoms within the tissue. Unlike positrons, these energetic photons do not "slow down"

but are attenuated. Because there is only one photon per event, electronic collimation is not possible, and a physical collimator must be added. Sensitivities are on the order of 10^{-14}–10^{-15} M for PET and 10^{-14} M for SPECT, and spatial resolution can reach 1.3 mm for PET and is sub-millimetric for SPECT [9]. PET and SPECT give information about physiological functions at the molecular level and are thus well suited to monitoring many vital processes, such as glucose metabolism, blood flow and perfusion, receptor-ligand binding rates, and oxygen utilization.

2.4. Optical imaging

Optical imaging is based on the detection of light passing through the tissues. Several major obstacles must be resolved for optical imaging, including surface reflectance, absorption, scattering (deviation of the photon from its original path) and autofluorescence. Absorption and autofluorescence are important factors in fluorescence imaging in the visible wavelengths (400–650 nm) but are less problematic in the near-infrared (NIR) (650–900 nm). Above 900 nm, however, water absorption is an issue because it prevents deep penetration of the light. Absorption is affected by the thickness and optical properties of the tissues. The body heterogeneity will compromise the linearity of measurements. In vivo, scattering of far-red photons affects the spatial resolution, which is dependent on the depth of observation. Spatial resolution is mainly affected by an animal's skin, which reflects light, but intravital microscopy greatly improves the resolution [1].

Light can be produced in live animals by two main types of reaction: bioluminescence (BLI) and fluorescence (for reviews see [10,11]). BLI is based on the self-emission of green to yellow light due to the oxidation of luciferin in the presence of luciferase enzymes (Firefly, Renilla, Aequoria…). BLI has minimal background signal and an excellent signal-to-noise ratio (SNR). Acquisition times range from seconds to minutes.

Two-dimensional fluorescence reflectance imaging (FRI) uses fluorescent probes to produce detectable signals (Fig. 1). In FRI, the sample is submitted to an NIR light (excitation) that can be absorbed by the fluorescent probe, which then emits light (fluoresces) at a longer wavelength as it returns from an excited electronic state to its ground level. The probe could be a protein (e.g., green fluorescent protein (GFP) or DsRed) present in genetically modified animals or cells or an exogenous fluorophore. Because these fluorescent proteins are not excitable in the far-red or NIR spectrum, but only in the 450–650 nm window, they are not well adapted to whole-body small animal imaging, and their detection is limited by depth (typically 1–2 mm). In contrast, some other fluorophores (such as cyanines, quantum dots, and lanthanides) can be exited in the far-red window, allowing deeper detection (typically 1–2 cm). Sensitivity is very good (10^{-12} M), spatial resolution varies from 100 μm in vitro to 2 mm in vivo and temporal resolution is in the range of milliseconds to seconds. However, 2D-FRI is highly surface-weighted, and quantification is at best semi-quantitative.

Recent development of 2D-FRI may allow its application in the clinic for improving cancer surgery. The Fluobeam® system (Fluoptics, Grenoble, France) uses a laser and small charge-coupled device (CCD) camera within a portable 2D-FRI system. It can function under the normal light of an operating room [12]. Another intraoperative device, the FLARE system (fluorescence-assisted resection and exploration), has already been used in preclinical trials [13–15].

Because of problems with absorption and autofluorescence, deep and absorbing tissues like lung, spleen or liver cannot be investigated non-invasively using 2D-FRI. Imaging these tissues requires the use of fluorescence molecular tomography (FMT) [16]. FMT provides 3D volumetric imaging, true quantification independent of depth, tissue optical properties and heterogeneity, and augmentation of the contrast by reducing the autofluorescence. Detecting deep events

Table 1
Characteristics of the different imaging devices.

Technique	Resolution	Depth	Time	Quantitative	Clinical use
CT	20 μm	No limit	Minutes	Yes	Yes
MRI	10 μm	No limit	Minutes to hours	Yes	Yes
PET	1–2 mm	No limit	Minutes to hours	Yes	Yes
SPECT	1 mm	No limit	Minutes to hours	Yes	Yes
FRI	μm to mm	<1 cm	Seconds	No	Yes
FMT	1 mm	<5 cm	Minutes to hours	Yes	Soon
BLI	1 mm	<1.5 cm	Minutes	No	No

A
2D-FRI
(Fluorescence Reflectance Imaging)

B
3D imaging
(Fluorescence Molecular Tomography)

C
Image guided surgery
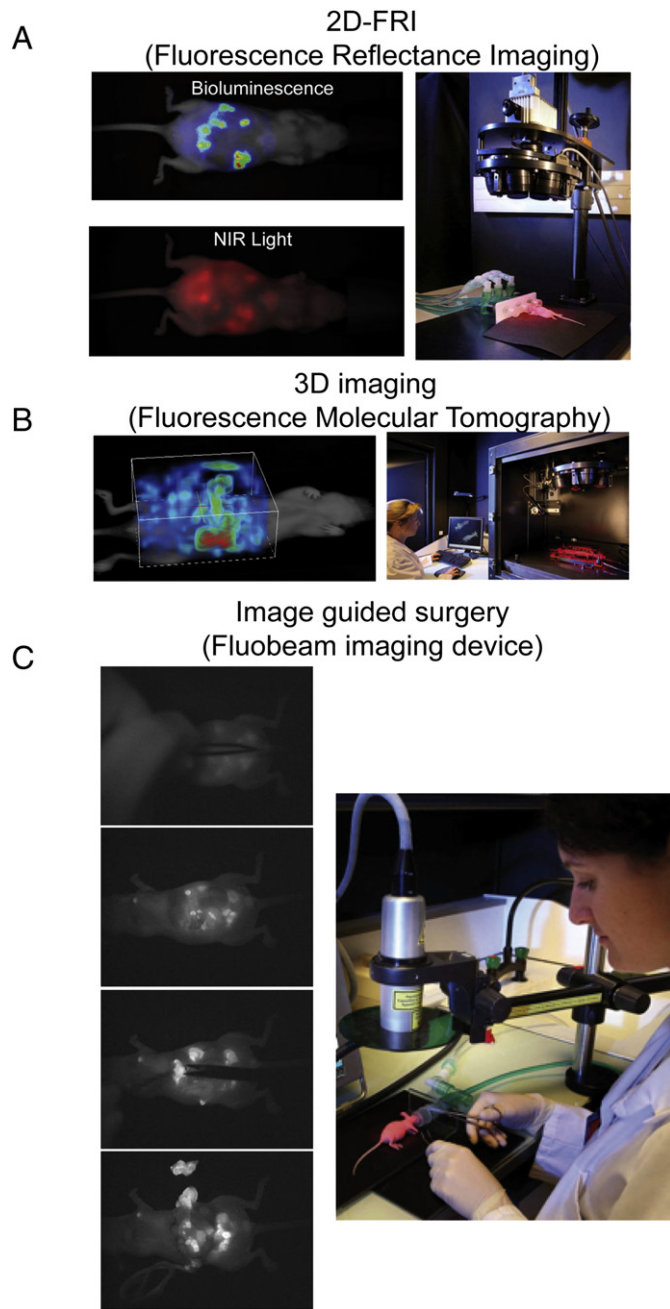#### (Fluobeam imaging device)

Fig. 1. Optical imaging of peritoneal carcinomatosis. (A) Tumor cells stably transfected with a luciferase reporter gene are injected into the peritoneal cavity of the mouse (top left image). The presence of small nodules is detected 12 days later using bioluminescence. The same nodules are also detected using 2D near-infrared fluorescence (bottom left image) due to the intravenous injection of 10 nmol Angiostamp (multimeric RGD compound described in [34–39,63–65]) the day before imaging using the 2D-FRI imaging system presented on the right. (B) Angiostamp-labeled nodules of the same animal can also be visualized in 3D using the tomographic system. (C) Optic-guided surgery can then be performed under near-infrared excitation using the Fluobeam device even when the surgical white light is illuminating the field of operation, allowing the surgeon to detect easily and remove all the labeled tumors as presented in the 4 consecutive images on the left.

requires transillumination to avoid autofluorescence [17]. Transillumination can be done using a simple optical bench adapted to continuous wave acquisitions [18–20]. The mouse is scanned with an NIR laser light, and the transmitted and emitted fluorescence are recorded allowing construction of a 3-D fluorescence map. Deeper imaging can be obtained using time-resolved imaging. Deeper imaging necessitates the use of expensive femtosecond pulsed lasers

and must be used in the time-resolved FDOT mode. Briefly, this process calculates and analyzes the time that each photon travels, whereas the photons are "simply" captured by the CCD as they arrive in continuous acquisition. This method will soon be transferred to the clinic for imaging deep events [21]. Recent work suggests that a fluorescent signal can be obtained in samples 2 to 5-cm thick, which could be sufficient, for example, for prostate imaging.

3. Fluorescent optical probes

As mentioned above, optical imaging of small animals requires the use of imaging devices and of fluorescent probes adapted to functional imaging. Several types of probes can be classified into three different categories, as summarized by R Weilssleider [22]. The simplest probes are usually large molecules that remain in circulation in the blood and can provide information about physiological processes, such as changes in blood volume, perfusion and angiogenesis. The second probe category targets a specific molecule, including receptors for somatostatin, epidermal growth factor (EGF), integrins, folate, or antigen-targeted antibodies, and can be used to visualize pathological tissues and/or monitor the expression level of a target. The third group of probes is composed of "smart probes" that undergo a change in optical properties when in contact with their targets (Fig. 2). These activatable probes are well adapted for detecting thio-reductases, proteases, such as matrix metalloproteinases (MMPs), cathepsins, caspases, or other enzymes and physicochemical parameters. In this chapter, we will focus on "targeted" and "activatable" probes; finally, we will describe the use of nanoparticles as optical imaging tools.

3.1. Receptor-targeted probes

Early diagnostics and image-guided tumor surgery are two key objectives of optical imaging. Kobayashi and colleagues developed several activatable probes and multicolor and multimodality imaging systems to enhance surgical outcomes. They demonstrated the feasibility of simultaneous visualization of two fluorophores using either a transfected cell line and an anti-HER2 antibody coupled with rhodamine G, or two antibodies labeled with two different fluorophores [23–25]. The next stage of development for this technique will concern the fluorophores themselves, as only one compound, indocyanin green (ICG), is currently approved for medical use.

Probes containing the Arg-Gly-Asp motif (RGD) have been intensively developed to follow expression of integrin $\alpha_v\beta_3$ [26], a protein that is expressed by the neo-endothelial cells that form tumor blood vessels and is also frequently overexpressed on tumor cells themselves, such as in lung cancers [27,28], melanomas [29,30], brain tumors [31] or breast cancers [32]. Because of the extraordinary potential of RGD derivatives as tumor targeting ligands, several teams have developed probes with improved receptor specificity and affinity. The first example, c(-RGDf[NMe]V), known as cilengitide, was developed through extensive work by Kessler et al. and has entered phase II trials for patients with glioblastoma. More recently, this group designed new molecules that could be even more specific and are capable of recognizing the $\alpha_v\beta_3$ or $\alpha_5\beta_1$ integrins [33]. RGD utility has also been greatly improved with the construction of scaffolds or polymers that allow multimeric presentation of the RGD triad. For example, our group developed a scaffold containing four copies of c(-RGDfK-) and compared its specificity *in vitro* and *in vivo* as well as its accumulation in tumors in $\alpha_v\beta_3$-positive tumor-bearing mice. The tetrameric RGD-probe showed a better affinity toward $\alpha_v\beta_3$, improved active internalization into the target cells and an augmented SNR *in vivo* compared to the monomeric molecule [34–39]. Because of their specific targeting properties, RGD probes can be used to monitor the efficacy of an anti-integrin or anti-angiogenic
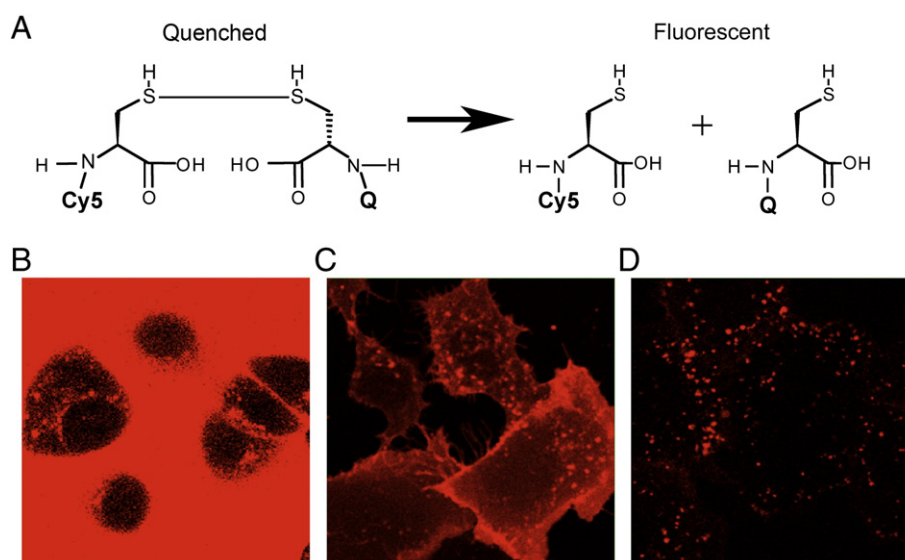
Fig. 2. Use of a quenched probe. (A) Schematic representation of the quenching system, containing a disulfide bridge to separate the quencher from the fluorescent cyanine 5 (Cy5) molecule. When the distance between the quencher and the Cy5 increases, the molecule becomes visible. (B) When the RAFT-RGD-Cy5 [35,37,39] probe is present in the culture medium without the quenching system, the cells are barely visible under the confocal microscope due to the surrounding fluorescence. (C) After removing the excess of RAFT-RGD-Cy5 from the medium, the cells are visible because the probes are attached to and internalized within the cell. (D) However, when a quenched probe is used, only the signal coming from the probe that is reduced during its internalization is visible, and the live cells can be observed even with a large excess of invisible quenched probe in the culture medium.

treatment non-invasively and in real time, as demonstrated in an orthotopic glioblastoma model [40]. In our laboratory, we also showed the utility of visualizing the multimeric RAFT-cRGD molecule using the portable intraoperative Fluobeam® imaging device to improved the quality and outcome of tumor surgery (Fig. 1) [12].

Monitoring the efficacy of recently developed anti-EGF receptor (EGFR) cancer treatments is of the utmost importance. To assess EGF binding/anti-EGF treatments efficacy and cell viability, anti-EGFR coupled with IRDye® 800 CW (LI-COR, NIR800) and annexin-V coupled with IRDye® 700DX (LI-COR, NIR700) were used to follow EGFR expression in colorectal tumors-bearing mice [41]. This study showed that anti-EGF-NIR800 accumulated more actively in tumors expressing high levels of EGFR and, annexin-V-NIR700 staining intensity was elevated in sensitive tumors treated with cetuximab compared to control groups. These imaging approaches may prove useful for serial, non-invasive monitoring of the biological effects of EGFR inhibition in preclinical studies and may also be adapted for clinical use. As described for cRGD, cyanine 5.5-labeled cetuximab has also been used to improve tumor resection and margin prevention in head and neck carcinomas [42].

3.2. Activatable molecules for fluorescent imaging

Optical imaging is the method of choice for functional, real-time, *in vivo* monitoring because it provides an "easy" approach for measuring enzymatic activities, thus enabling researchers to follow, for example, the activation of signal transduction pathways, target gene expression and drug–target interactions [43]. It also allows the *in vivo* analysis of drug efficacy and pharmacodynamic properties.

Several proteases are overexpressed or activated during cancer progression and are thus attractive targets for the so-called "smart" probes, also known as activatable molecules (Fig. 2). Activatable means that a change in signal intensity or wavelength can be detected in response to the interaction of the probe with its target [19,44]. Activatable molecules have several advantages, including minimal non-specific background and improved contrast in the targeted organ [43,45,46]. Proteases were the first enzymes to be targeted in this way, as described for cathepsins (cathepsin B and cathepsin D for cancer progression and cathepsin K for the detection of osteoclasts), caspases-1 and -3 (indicators of apoptosis) and MMPs 2, -7, -9, and

-14 (inflammation and cancer) [22,47–49]. Because the signals produced by these probes are a direct function of their biological activity, smart probes can be used to measure the activity of a drug on its target [50–54].

One of the first NIR activatable probes, described by Weissleder et al., is a polymer of poly-L-lysine and methoxypolyethylene glycol succinate [55]. This probe has a long circulation time, and its fluorescence is quenched in the presence of a high concentration of fluorescent molecules. A detectable NIR signal is (re)-generated when these self-quenched molecules are digested by lysosomal proteases after internalization in the target tumor cells, allowing the detection of sub-millimeter-sized nodules. A similar strategy was used to detect cathepsins B, K, L, and S in cardiac pathologies [56] and image cancer in mouse model of adenoma of the gastrointestinal track [57], or rhabdomyosarcoma [58].

In vivo monitoring of apoptosis is also of great interest. Using a self-quenched caspase-activatable peptide (TcapQ647), Bullok et al. measured *in vivo* apoptosis that was induced by bacterial infection. Activation of the probe was confirmed by *ex-vivo* TUNEL analysis of the tissues and by detection of activated caspase-3 [59]. However, good enzymatic specificity is still an issue facing this technique. For example, it is difficult to design a caspase-specific probe that has low cross-reactivity for cathepsins or legumain. To circumvent this problem, Edgington et al. developed NIR activity-based molecules that form permanent covalent bonds with target proteases, based on acyloxymethyl ketone (AOMK) probes. These probes can be used to monitor early stages of apoptosis using whole-body, non-invasive optical imaging, as demonstrated in human colorectal tumor-bearing mice [60].

The search for new drugs capable of inhibiting receptor tyrosine kinases (RTK) such as EGFR is currently a major issue for cancer treatment. To assess drug efficiency against EGFR, a novel bioluminescent-based approach using a bifragment luciferase reconstitution system was recently reported [61]. EGFR and its interacting partner proteins were fused to the NH2- and COOH-terminal fragments of firefly luciferase. This method allowed the identification and quantification of EGFR activation in mice before and after anti-EGFR treatments, such as gefitinib or radiotherapy. This technique is a promising tool that could enhance the preclinical evaluation of novel RTK-targeted therapeutics.

Other activatable compounds have been developed to target viable cancer cells. Urano et al. made a pH-activatable probe coupled to the anti-HER-2 monoclonal antibody trastuzumab. In mice bearing subcutaneous tumors, the probe was highly specific for HER-2-positive tumors with a minimal background signal. Because the energy-consuming proton pumps maintain an acidic pH in lysosomes, only viable HER-2-positive cancer cells showed a high signal [62]. The intracellular redox environments of viable cells can also be used to design probes in which fluorescence will be released after rupture of a disulfide bridge during following internalization. Our group used this method to design RGD-based targeted probes that allow the tracking of a pro-apoptotic toxic peptide released within the target cells [63–66].

3.3. Nanoparticles developed for in vivo applications

During the last few years, a wide variety of nanoparticles were developed as contrast agents for *in vivo* fluorescence imaging applications. Due to their size, these particles offer new structural and optical properties. They have better signal intensity than organic fluorophores, enabling detection of weakly expressed targeted biomarkers. In addition, because of their relatively large surface area, nanoparticles can accommodate multiple probes, enabling multivalent targeting of several biomarkers and thus increasing the affinity of each individual probe. All of these properties make nanoparticles good candidates for biomedical imaging, therapeutic applications or a combination of both (theranostics).

Quantum dots (QDs) are the most extensively described and studied nanoparticles [67–76]. These small nanocrystals are made of semiconductive material and have an emission color that can be precisely tuned by adjusting their composition and size [77]. They can thus be used across a wide spectrum, from the ultraviolet to the NIR and are also photostable and extremely bright [78]. Recently, QDs were also encapsulated in phospholipid micelles to image tumors [79,80]. The encapsulation of QDs enhanced their biodistribution and their passive accumulation in tumors. Various nanoparticles have also been developed for *in vivo* fluorescence imaging applications: these nanoparticles include gold nanoparticles [81,82], hybrid nanoparticles [83–86], C dots [87], lipid nanoparticles [88], liposomes [89], polymeric nanoparticles [90,91], and biodegradable luminescent porous silicon nanoparticles [92].

Several applications have been developed using these new contrast agents. In 2004, Kim et al. demonstrated that QDs translocated to sentinel lymph nodes after intra-dermal injection, likely due to a combination of passive flow in lymphatic vessels and active migration of dendritic cells that had engulfed the nanoparticles [70]. This application could have a great clinical impact, enabling surgeons to rapidly identify and excise draining lymph nodes from tumors for staging cancer using optical guided surgery [93]. The major limitation of QDs is their possible toxicity, which thus far precludes their use in humans. A recent study found no appreciable toxicity of QD, even after their breakdown *in vivo* [94]; however, because of their different chemical formulations and nanoparticle structures, the absence of toxicity of each type of QD, as well as that of each of its byproducts, must be very carefully investigated. Currently, this technique has been used to localize various cancers in animal models, including subcutaneous tumors [95], lungs [71,72], esophagus [73], and head and neck [76].

The key challenge for *in vivo* imaging applications is to develop nanoparticles with an optimized biodistribution. Several studies have shown the particular importance of particle size, PEGylation and surface coating. These properties affect the mean of accumulation in and elimination from tumors through the enhanced permeability and retention (EPR) effect (Fig. 3) [83,95,96]. Indeed, during tumor-induced angiogenesis, blood vessels are abnormal and present large pores, allowing the extravasation of macromolecules up to 400 nm in
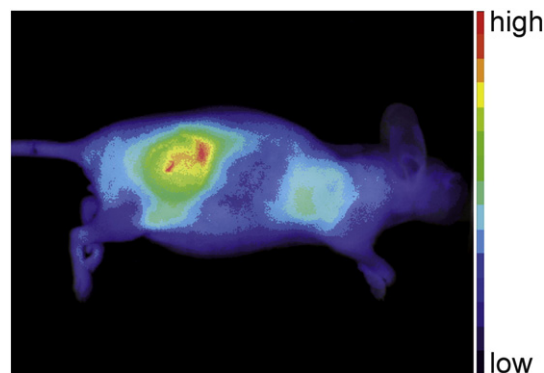

Fig. 3. The EPR effect allows passive targeting of a nanoparticle into a subcutaneous tumor. Intravenous injection of a solid PEG2000-coated particle in a *nude* mouse bearing a subcutaneous tumor. Fluorescence image obtained 24 h after injection shows the accumulation of the nanoparticle in the tumor, due to the enhanced permeability and retention (EPR) effect.

size, that can accumulate in the tumor microenvironment [97]. This EPR effect has inspired the development of a variety of nanoparticles to treat and image tumors. Several groups have studied the biodistribution of hydrophobically modified glycol chitosan nanoparticles loaded with cisplatin, camptothecin or paclitaxel by *in vivo* NIR imaging [98–100]. These groups have found a passive but specific accumulation in subcutaneous tumors due to the EPR effect, as well as increased effectiveness of encapsulated drugs compared to free drugs.

To improve the tumor targeting selectivity, specific ligands can be grafted onto the surface of nanoparticles. Again, one of the most commonly described ligands for tumor targeting is the RGD peptide [69,75,101], though several specific other tumor ligands have also been investigated. *In vivo* targeted imaging was demonstrated in a mouse model, using a copolymer functionalized QD conjugated to an antibody that targets a prostate-specific membrane antigen [68]. Gold nanoparticles labeled with anti-EGFR monoclonal antibodies also have a large range of potential applications, from the cellular to the animal levels [81]. Lee et al. [102] recently developed a multifunctional gold nanoprobe for sensitive detection of reactive oxygen species (ROS) and hyaluronidase, which could be used for localized detection of hyaluronic acid degradation due to the diseases such as rheumatoid arthritis and metastatic tumors. Yang et al. described iron oxide nanoparticles that target urokinase plasminogen activator (uPA) receptor and demonstrated their usefulness in detecting breast and pancreatic cancer [91,103].

Finally, nanoprobes can also be powerful tools for evaluating the efficiency of targeted cancer therapies. Medarova et al. [104] described a tumor-specific contrast agent (iron oxide nanoparticles labeled with Cy5.5 dye) targeting underglycolated mucin 1 (uMUC-1), a tumor antigen present on more than 90% of breast cancers and predictive of chemotherapeutic response. After doxorubicin treatment, nanoparticle probes were present at a lower level in the treated tumors compared to untreated tumors, reflecting the reduced expression of uMUC-1. To confirm these findings, similar results were obtained using *in vivo* fluorescence imaging and MRI. The same kind of nanoparticle was also used to deliver small interfering RNA (siRNA) *in vivo* and track their successful delivery by non-invasive imaging [105].

In conclusion, nano-sized contrast agents offer several advantages over conventional agents because they can be passively targeted to the tumors via the EPR effect or actively targeted by specific ligands. Most importantly, nanoparticles offer multifunctionality, such as combining imaging and drug (or siRNA) delivery or, providing dual-modality imaging that combines NIR and either MRI or PET [106]. Thus, these nanoparticles promise great versatility in the detection and treatment of diseases.

4. Conclusion

Optical imaging is an inexpensive, easy-to-use, and non-radiative tool that can provide rapid semi-qualitative (2D), quantitative (3D), and functional information from the cellular to the several centimeter scale. Fluorescence molecular tomography is the preferred method for quantifying protein levels and enzymatic activities. 2D-fluorescent reflectance optical imaging is poised to be the premier approach in molecular imaging, especially for researchers who are not specialists in medical imaging or who do not have access to a nuclear medicine facility or very expensive magnets. However, the future of cancer imaging in mice will rely on the development of a large collection of highly specific tracers or smart contrasting agents. Coupling high-resolution methods like micro-CT or MRI with highly sensitive techniques adapted to functional imaging, such as PET, SPECT or optical imaging, will soon open new frontiers in the study of cancer in small animals and will provide efficient tools for evaluating new treatments. Importantly, a major bottleneck that inhibits the widespread application and generation of these probes concerns the use of NIR fluorophores in human clinical trials by legal agencies. In response to this issue, the FDA recently established the Process Analytical Technologies initiative, which will certainly facilitate the manufacture and use of NIR probes.

References

[1] M. Baker, Whole-animal imaging: the whole picture, Nature 463 (2010) 977–980.

[2] D.W. Holdsworth, M.M. Thornton, Micro-CT in small animal and specimen imaging, Trends Biotechnol. 20 (2002) s34–s39.

[3] P.J. Cassidy, G.K. Radda, Molecular imaging perspectives, J. R. Soc. Interface 2 (2005) 133–144.

[4] A. Louie, Design and characterization of magnetic resonance imaging gene reporters, Methods Mol. Med. 124 (2006) 401–417.

[5] T. Barrett, H. Kobayashi, M. Brechbiel, P.L. Choyke, Macromolecular MRI contrast agents for imaging tumor angiogenesis, Eur. J. Radiol. 60 (2006) 353–366.

[6] M. Beaumont, B. Lemasson, R. Farion, C. Segebarth, C. Remy, E.L. Barbier, Characterization of tumor angiogenesis in rat brain using iron-based vessel size index MRI in combination with gadolinium-based dynamic contrast-enhanced MRI, J. Cereb. Blood Flow Metab. 29 (2009) 1714–1726.

[7] C.A. Cuenod, L. Fournier, D. Balvay, J.M. Guinebretiere, Tumor angiogenesis: pathophysiology and implications for contrast-enhanced MRI and CT assessment, Abdom. Imaging 31 (2006) 188–193.

[8] C.S. Levin, Primer on molecular imaging technology, Eur. J. Nucl. Med. Mol. Imaging 32 (Suppl 2) (2005) S325–S345.

[9] A.F. Chatziioannou, S.R. Cherry, Y. Shao, R.W. Silverman, K. Meadors, T.H. Farquhar, M. Pedarsani, M.E. Phelps, Performance evaluation of microPET: a high-resolution lutetium oxyorthosilicate PET scanner for animal imaging, J. Nucl. Med. 40 (1999) 1164–1175.

[10] D.K. Welsh, S.A. Kay, Bioluminescence imaging in living organisms, Curr. Opin. Biotechnol. 16 (2005) 73–78.

[11] C. Bremer, V. Ntziachristos, R. Weissleder, Optical-based molecular imaging: contrast agents and potential medical applications, Eur. Radiol. 13 (2003) 231–243.

[12] M. Kéramidas, V. Josserand, C.A. Righini, C. Wenk, C. Coll, J.L. Faure, Intraoperative near-infrared image-guided surgery of peritoneal carcinomatosis in a preclinical mouse model, British Journal of Surgery (2010) (Mar. 22, Electronic publication ahead of print), doi:10.1002/bjs.6986.

[13] S.L. Troyan, V. Kianzad, S.L. Gibbs-Strauss, S. Gioux, A. Matsui, R. Oketokoun, L. Ngo, A. Khamene, F. Azar, J.V. Frangioni, The FLARE intraoperative near-infrared fluorescence imaging system: a first-in-human clinical trial in breast cancer sentinel lymph node mapping, Ann. Surg. Oncol. 16 (10) (2009) 2943–2952.

[14] A. Nakayama, F. del Monte, R.J. Hajjar, J.V. Frangioni, Functional near-infrared fluorescence imaging for cardiac surgery and targeted gene therapy, Mol. Imaging 1 (2002) 365–377.

[15] J.V. Frangioni, New technologies for human cancer imaging, J. Clin. Oncol. 26 (2008) 4012–4021.

[16] V. Ntziachristos, C. Bremer, E.E. Graves, J. Ripoll, R. Weissleder, In vivo tomographic imaging of near-infrared fluorescent probes, Mol. Imaging 1 (2002) 82–88.

[17] A. Koenig, L. Herve, V. Josserand, M. Berger, J. Boutet, A. Da Silva, J.M. Dinten, P. Peltie, J.L. Coll, P. Rizo, In vivo mice lung tumor follow-up with fluorescence diffuse optical tomography, J. Biomed. Opt. 13 (2008) 011008.

[18] A. Da Silva, J.M. Dinten, J.L. Coll, P. Rizo, From bench-top small animal diffuse optical tomography towards clinical imaging, Conf. Proc. IEEE Eng. Med. Biol. Soc. (2007) 526–529.

[19] V. Ntziachristos, C.H. Tung, C. Bremer, R. Weissleder, Fluorescence molecular tomography resolves protease activity in vivo, Nat. Med. 8 (2002) 757–760.

[20] X. Montet, V. Ntziachristos, J. Grimm, R. Weissleder, Tomographic fluorescence mapping of tumor targets, Cancer Res. 65 (2005) 6330–6336.

[21] J. Boutet, L. Herve, M. Debourdeau, L. Guyon, P. Peltie, J.M. Dinten, L. Saroul, F. Duboeuf, D. Vray, Bimodal ultrasound and fluorescence approach for prostate cancer diagnosis, J. Biomed. Opt. 14 (2009) 064001.

[22] R. Weissleder, V. Ntziachristos, Shedding light onto live molecular targets, Nat. Med. 9 (2003) 123–128.

[23] M. Longmire, N. Kosaka, M. Ogawa, P.L. Choyke, H. Kobayashi, Multicolor in vivo targeted imaging to guide real-time surgery of HER2-positive micrometastases in a two-tumor coincident model of ovarian cancer, Cancer Sci. 100 (2009) 1099–1104.

[24] M. Ogawa, C.A. Regino, P.L. Choyke, H. Kobayashi, In vivo target-specific activatable near-infrared optical labeling of humanized monoclonal antibodies, Mol. Cancer Ther. 8 (2009) 232–239.

[25] M. Ogawa, N. Kosaka, P.L. Choyke, H. Kobayashi, In vivo molecular imaging of cancer with a quenching near-infrared fluorescent probe using conjugates of monoclonal antibodies and indocyanine green, Cancer Res. 69 (2009) 1268–1272.

[26] X. Chen, P.S. Conti, R.A. Moats, In vivo near-infrared fluorescence imaging of integrin alphavbeta3 in brain tumor xenografts, Cancer Res. 64 (2004) 8009–8014.

[27] X. Chen, E. Sievers, Y. Hou, R. Park, M. Tohme, R. Bart, R. Bremner, J.R. Bading, P.S. Conti, Integrin alpha v beta 3-targeted imaging of lung cancer, Neoplasia 7 (2005) 271–279.

[28] T. Sato, K. Konishi, H. Kimura, K. Maeda, K. Yabushita, M. Tsuji, A. Miwa, Vascular integrin beta 3 and its relation to pulmonary metastasis of colorectal carcinoma, Anticancer Res. 21 (2001) 643–647.

[29] K.R. Gehlsen, G.E. Davis, P. Sriramarao, Integrin expression in human melanoma cells with differing invasive and metastatic properties, Clin. Exp. Metastasis 10 (1992) 111–120.

[30] R.E. Seftor, E.A. Seftor, K.R. Gehlsen, W.G. Stetler-Stevenson, P.D. Brown, E. Ruoslahti, M.J. Hendrix, Role of the alpha v beta 3 integrin in human melanoma cell invasion, Proc. Natl. Acad. Sci. U. S. A. 89 (1992) 1557–1561.

[31] C.L. Gladson, D.A. Cheresh, Glioblastoma expression of vitronectin and the alpha v beta 3 integrin. Adhesion mechanism for transformed glial cells, J. Clin. Invest. 88 (1991) 1924–1932.

[32] M. Rolli, E. Fransvea, J. Pilch, A. Saven, B. Felding-Habermann, Activated integrin alphavbeta3 cooperates with metalloproteinase MMP-9 in regulating migration of metastatic breast cancer cells, Proc. Natl. Acad. Sci. U. S. A. 100 (2003) 9482–9487.

[33] D. Heckmann, A. Meyer, L. Marinelli, G. Zahn, R. Stragies, H. Kessler, Probing integrin selectivity: rational design of highly active and selective ligands for the alpha5beta1 and alphavbeta3 integrin receptor, Angew. Chem. Int. Ed. Engl. 46 (2007) 3571–3574.

[34] D. Boturyn, J.L. Coll, E. Garanger, M.C. Favrot, P. Dumy, Template assembled cyclopeptides as multimeric system for integrin targeting and endocytosis, J. Am. Chem. Soc. 126 (2004) 5730–5739.

[35] L. Sancey, E. Garanger, S. Foillard, G. Schoehn, A. Hurbin, C. Albiges-Rizo, D. Boturyn, C. Souchier, A. Grichine, P. Dumy, J.L. Coll, Clustering and internalization of integrin alphavbeta3 with a tetrameric RGD-synthetic peptide, Mol. Ther. 17 (2009) 837–843.

[36] Z.H. Jin, V. Josserand, S. Foillard, D. Boturyn, P. Dumy, M.C. Favrot, J.L. Coll, In vivo optical imaging of integrin alphaV-beta3 in mice using multivalent or monovalent cRGD targeting vectors, Mol. Cancer 6 (2007) 41.

[37] Z.H. Jin, V. Josserand, J. Razkin, E. Garanger, D. Boturyn, M.C. Favrot, P. Dumy, J.L. Coll, Noninvasive optical imaging of ovarian metastases using Cy5-labeled RAFT-c(-RGDfK-)4, Mol. Imaging 5 (2006) 188–197.

[38] L. Sancey, V. Ardisson, L.M. Riou, M. Ahmadi, D. Marti-Batlle, D. Boturyn, P. Dumy, D. Fagret, C. Ghezzi, J.P. Vuillez, In vivo imaging of tumour angiogenesis in mice with the alpha(v)beta (3) integrin-targeted tracer 99mTc-RAFT-RGD, Eur. J. Nucl. Med. Mol. Imaging 34 (2007) 2037–2047.

[39] L. Sancey, S. Dufort, V. Josserand, M. Keramidas, C.A. Righini, C. Rome, A.C. Faure, S. Foillard, S. Roux, D. Boturyn, O. Tillement, A. Koenig, J. Boutet, P. Rizo, P. Dumy, J.L. Coll, Drug development in oncology assisted by noninvasive optical imaging, Int. J. Pharm. 379 (2009) 309–316.

[40] A.R. Hsu, L.C. Hou, A. Veeravagu, J.M. Greve, H. Vogel, V. Tse, X. Chen, In vivo near-infrared fluorescence imaging of integrin alphavbeta3 in an orthotopic glioblastoma model, Mol. Imaging Biol. 8 (2006) 315–323.

[41] H.C. Manning, N.B. Merchant, A.C. Foutch, J.M. Virostko, S.K. Wyatt, C. Shah, E.T. McKinley, J. Xie, N.J. Mutic, M.K. Washington, B. LaFleur, M.N. Tantawy, T.E. Peterson, M.S. Ansari, R.M. Baldwin, M.L. Rothenberg, D.J. Bornhop, J.C. Gore, R.J. Coffey, Molecular imaging of therapeutic response to epidermal growth factor receptor blockade in colorectal cancer, Clin. Cancer Res. 14 (2008) 7413–7422.

[42] E.L. Rosenthal, B.D. Kulbersh, T. King, T.R. Chaudhuri, K.R. Zinn, Use of fluorescent labeled anti-epidermal growth factor receptor antibody to image head and neck squamous cell carcinoma xenografts, Mol. Cancer Ther. 6 (2007) 1230–1238.

[43] S.B. Raymond, J. Skoch, I.D. Hills, E.E. Nesterov, T.M. Swager, B.J. Bacskai, Smart optical probes for near-infrared fluorescence imaging of Alzheimer's disease pathology, Eur. J. Nucl. Med. Mol. Imaging 35 (Suppl 1) (2008) S93–S98.

[44] M.C. Pierce, D.J. Javier, R. Richards-Kortum, Optical contrast agents and imaging systems for detection and diagnosis of cancer, Int. J. Cancer 123 (2008) 1979–1990.

[45] M. Ogawa, C.A. Regino, J. Seidel, M.V. Green, W. Xi, M. Williams, N. Kosaka, P.L. Choyke, H. Kobayashi, Dual-modality molecular imaging using antibodies

labeled with activatable fluorescence and a radionuclide for specific and quantitative targeted cancer detection, Bioconjug. Chem. 20 (2009) 2177–2184.

[46] D.R. Elias, D.L. Thorek, A.K. Chen, J. Czupryna, A. Tsourkas, In vivo imaging of cancer biomarkers using activatable molecular probes, Cancer Biomark. 4 (2008) 287–305.

[47] C. Bremer, V. Ntziachristos, R. Weissleder, Optical-based molecular imaging: contrast agents and potential medical applications, Eur. Radiol. 13 (2003) 231–243.

[48] J.L. Figueiredo, H. Alencar, R. Weissleder, U. Mahmood, Near infrared thoracoscopy of tumoral protease activity for improved detection of peripheral lung cancer, Int. J. Cancer 118 (2006) 2672–2677.

[49] G. Blum, G. von Degenfeld, M.J. Merchant, H.M. Blau, M. Bogyo, Noninvasive optical imaging of cysteine protease activity using fluorescently quenched activity-based probes, Nat. Chem. Biol. 3 (2007) 668–677.

[50] F. Zhou, D. Xing, S. Wu, W.R. Chen, Intravital imaging of tumor apoptosis with FRET probes during tumor therapy, Mol. Imaging Biol. 12 (1) (2010) 63–70.

[51] A. Sierra, Animal models of breast cancer for the study of pathogenesis and therapeutic insights, Clin. Transl. Oncol. 11 (2009) 721–727.

[52] J. Ripoll, V. Ntziachristos, C. Cannet, A.L. Babin, R. Kneuer, H.U. Gremlich, N. Beckmann, Investigating pharmacology in vivo using magnetic resonance and optical imaging, Drugs R D 9 (2008) 277–306.

[53] D.A. Torigian, S.S. Huang, M. Houseni, A. Alavi, Functional imaging of cancer with emphasis on molecular techniques, CA Cancer J. Clin. 57 (2007) 206–224.

[54] R.L. Scherer, M.N. VanSaun, J.O. McIntyre, L.M. Matrisian, Optical imaging of matrix metalloproteinase-7 activity in vivo using a proteolytic nanobeacon, Mol. Imaging 7 (2008) 118–131.

[55] R. Weissleder, C.H. Tung, U. Mahmood, A. Bogdanov Jr., In vivo imaging of tumors with protease-activated near-infrared fluorescent probes, Nat. Biotechnol. 17 (1999) 375–378.

[56] M. Nahrendorf, D.E. Sosnovik, P. Waterman, F.K. Swirski, A.N. Pande, E. Aikawa, J. L. Figueiredo, M.J. Pittet, R. Weissleder, Dual channel optical tomographic imaging of leukocyte recruitment and protease activity in the healing myocardial infarct, Circ. Res. 100 (2007) 1218–1225.

[57] H. Zhang, D. Morgan, G. Cecil, A. Burkholder, N. Ramocki, B. Scull, P.K. Lund, Biochromoendoscopy: molecular imaging with capsule endoscopy for detection of adenomas of the GI tract, Gastrointest. Endosc. 68 (2008) 520–527.

[58] S. Kossodo, M. Pickarski, S.A. Lin, A. Gleason, R. Gaspar, C. Buono, G. Ho, A. Blusztajn, G. Cuneo, J. Zhang, J. Jensen, R. Hargreaves, P. Coleman, G. Hartman, M. Rajopadhye, L.T. Duong, C. Sur, W. Yared, J. Peterson, B. Bednar, Dual in vivo quantification of integrin-targeted and protease-activated agents in cancer using fluorescence molecular tomography (FMT), Mol. Imaging Biol. (2009) (Dec. 4, Electronic publication ahead of print), doi:10.1007/s11307-009-0279-z.

[59] K.E. Bullok, D. Maxwell, A.H. Kesarwala, S. Gammon, J.L. Prior, M. Snow, S. Stanley, D. Piwnica-Worms, Biochemical and in vivo characterization of a small, membrane-permeant, caspase-activatable far-red fluorescent peptide for imaging apoptosis, Biochemistry 46 (2007) 4055–4065.

[60] L.E. Edgington, A.B. Berger, G. Blum, V.E. Albrow, M.G. Paulick, N. Lineberry, M. Bogyo, Noninvasive optical imaging of apoptosis by caspase-targeted activity-based probes, Nat. Med. 15 (2009) 967–973.

[61] W. Li, F. Li, Q. Huang, B. Frederick, S. Bao, C.Y. Li, Noninvasive imaging and quantification of epidermal growth factor receptor kinase activation in vivo, Cancer Res. 68 (2008) 4990–4997.

[62] Y. Urano, D. Asanuma, Y. Hama, Y. Koyama, T. Barrett, M. Kamiya, T. Nagano, T. Watanabe, A. Hasegawa, P.L. Choyke, H. Kobayashi, Selective molecular imaging of viable cancer cells with pH-activatable fluorescence probes, Nat. Med. 15 (2009) 104–109.

[63] S. Foillard, L. Sancey, J.L. Coll, D. Boturyn, P. Dumy, Targeted delivery of activatable fluorescent pro-apoptotic peptide into live cells, Org. Biomol. Chem. 7 (2009) 221–224.

[64] Z.H. Jin, J. Razkin, V. Josserand, D. Boturyn, A. Grichine, I. Texier, M.C. Favrot, P. Dumy, J.L. Coll, In vivo noninvasive optical imaging of receptor-mediated RGD internalization using self-quenched Cy5-labeled RAFT-c(-RGDfK-)(4), Mol. Imaging 6 (2007) 43–55.

[65] J. Razkin, V. Josserand, D. Boturyn, Z.H. Jin, P. Dumy, M. Favrot, J.L. Coll, I. Texier, Activatable fluorescent probes for tumour-targeting imaging in live mice, ChemMedChem 1 (2006) 1069–1072.

[66] I. Texier-Nogues, J. Razkin, V. Josserand, D. Boturyn, P. Dumy, J.L. Coll, P. Rizo, Activatable probes for non-invasive small animal fluorescence imaging, Nucl. Instrum. Methods Phys. Res. A (2007) 165–168.

[67] B. Dubertret, P. Skourides, D.J. Norris, V. Noireaux, A.H. Brivanlou, A. Libchaber, In vivo imaging of quantum dots encapsulated in phospholipid micelles, Science 298 (2002) 1759–1762.

[68] X. Gao, Y. Cui, R.M. Levenson, L.W. Chung, S. Nie, In vivo cancer targeting and imaging with semiconductor quantum dots, Nat. Biotechnol. 22 (2004) 969–976.

[69] W. Cai, D.W. Shin, K. Chen, O. Gheysens, Q. Cao, S.X. Wang, S.S. Gambhir, X. Chen, Peptide-labeled near-infrared quantum dots for imaging tumor vasculature in living subjects, Nano Lett. 6 (2006) 669–676.

[70] S. Kim, Y.T. Lim, E.G. Soltesz, A.M. De Grand, J. Lee, A. Nakayama, J.A. Parker, T. Mihaljevic, R.G. Laurence, D.M. Dor, L.H. Cohn, M.G. Bawendi, J.V. Frangioni, Near-infrared fluorescent type II quantum dots for sentinel lymph node mapping, Nat. Biotechnol. 22 (2004) 93–97.

[71] E.G. Soltesz, S. Kim, R.G. Laurence, A.M. DeGrand, C.P. Parungo, D.M. Dor, L.H. Cohn, M.G. Bawendi, J.V. Frangioni, T. Mihaljevic, Intraoperative sentinel lymph node mapping of the lung using near-infrared fluorescent quantum dots, Ann. Thorac. Surg. 79 (2005) 269–277 discussion 269–277.

[72] C.P. Parungo, Y.L. Colson, S.W. Kim, S. Kim, L.H. Cohn, M.G. Bawendi, J.V. Frangioni, Sentinel lymph node mapping of the pleural space, Chest 127 (2005) 1799–1804.

[73] C.P. Parungo, S. Ohnishi, S.W. Kim, S. Kim, R.G. Laurence, E.G. Soltesz, F.Y. Chen, Y. L. Colson, L.H. Cohn, M.G. Bawendi, J.V. Frangioni, Intraoperative identification of esophageal sentinel lymph nodes with near-infrared fluorescence imaging, J. Thorac. Cardiovasc. Surg. 129 (2005) 844–850.

[74] B. Ballou, L.A. Ernst, S. Andreko, T. Harper, J.A. Fitzpatrick, A.S. Waggoner, M.P. Bruchez, Sentinel lymph node imaging using quantum dots in mouse tumor models, Bioconjug. Chem. 18 (2007) 389–396.

[75] W. Cai, X. Chen, Preparation of peptide-conjugated quantum dots for tumor vasculature-targeted imaging, Nat. Protoc. 3 (2008) 89–96.

[76] H. Kobayashi, M. Ogawa, N. Kosaka, P.L. Choyke, Y. Urano, Multicolor imaging of lymphatic function with two nanomaterials: quantum dot-labeled cancer cells and dendrimer-based optical agents, Nanomed 4 (2009) 411–419.

[77] L.A. Bentolila, Y. Ebensteinn, S. Weiss, Quantum dots for in vivo small-animal imaging, J. Nucl. Med. 50 (2009) 493–496.

[78] B. Mahler, P. Spinicelli, S. Buil, X. Quelin, J.P. Hermier, B. Dubertret, Towards non-blinking colloidal quantum dots, Nat. Mater. 7 (2008) 659–664.

[79] O. Carion, B. Mahler, T. Pons, B. Dubertret, Synthesis, encapsulation, purification and coupling of single quantum dots in phospholipid micelles for their use in cellular and in vivo imaging, Nat. Protoc. 2 (2007) 2383–2390.

[80] A. Papagiannaros, T. Levchenko, W. Hartner, D. Mongayt, V. Torchilin, Quantum dots encapsulated in phospholipid micelles for imaging and quantification of tumors in the near-infrared region, Nanomedicine 5 (2009) 216–224.

[81] J. Aaron, N. Nitin, K. Travis, S. Kumar, T. Collier, S.Y. Park, M. Jose-Yacaman, L. Coghlan, M. Follen, R. Richards-Kortum, K. Sokolov, Plasmon resonance coupling of metal nanoparticles for molecular imaging of carcinogenesis in vivo, J. Biomed. Opt. 12 (2007) 034007.

[82] P. Puvanakrishnan, J. Park, P. Diagaradjane, J.A. Schwartz, C.L. Coleman, K.L. Gill-Sharp, K.L. Sang, J.D. Payne, S. Krishnan, J.W. Tunnell, Near-infrared narrow-band imaging of gold/silica nanoshells in tumors, J. Biomed. Opt. 14 (2009) 024044.

[83] A.C. Faure, S. Dufort, V. Josserand, P. Perriat, J.L. Coll, S. Roux, O. Tillement, Control of the in vivo biodistribution of hybrid nanoparticles with different poly (ethylene glycol) coatings, Small 5 (2009) 2565–2575.

[84] C. Chen, J. Peng, H.S. Xia, G.F. Yang, Q.S. Wu, L.D. Chen, L.B. Zeng, Z.L. Zhang, D.W. Pang, Y. Li, Quantum dots-based immunofluorescence technology for the quantitative determination of HER2 expression in breast cancer, Biomaterials 30 (2009) 2912–2918.

[85] C. Yang, N. Ding, Y. Xu, X. Qu, J. Zhang, C. Zhao, L. Hong, Y. Lu, G. Xiang, Folate receptor-targeted quantum dot liposomes as fluorescence probes, J. Drug Target. 17 (2009) 502–511.

[86] C.H. Yang, S.H. Yang, C.S. Hsu, Solution-processable phosphorescent to organic light-emitting diodes based on chromophoric amphiphile/silica nanocomposite, Nanotechnology 20 (2009) 315601.

[87] A.A. Burns, J. Vider, H. Ow, E. Herz, O. Penate-Medina, M. Baumgart, S.M. Larson, U. Wiesner, M. Bradbury, Fluorescent silica nanoparticles with efficient urinary excretion for nanomedicine, Nano Lett. 9 (2009) 442–448.

[88] I. Texier, M. Goutayer, A. Da Silva, L. Guyon, N. Djaker, V. Josserand, E. Neumann, J. Bibette, F. Vinet, Cyanine-loaded lipid nanoparticles for improved in vivo fluorescence imaging, J. Biomed. Opt. 14 (2009) 054005.

[89] K.C. Weng, C.O. Noble, B. Papahadjopoulos-Sternberg, F.F. Chen, D.C. Drummond, D. B. Kirpotin, D. Wang, Y.K. Hom, B. Hann, J.W. Park, Targeted tumor cell internalization and imaging of multifunctional quantum dot-conjugated immunoliposomes in vitro and in vivo, Nano Lett. 8 (2008) 2851–2857.

[90] A. Almutairi, R. Rossin, M. Shokeen, A. Hagooly, A. Ananth, B. Capoccia, S. Guillaudeu, D. Abendschein, C.J. Anderson, M.J. Welch, J.M. Frechet, Biodegradable dendritic positron-emitting nanoprobes for the noninvasive imaging of angiogenesis, Proc. Natl. Acad. Sci. U. S. A. 106 (2009) 685–690.

[91] L. Yang, H. Mao, Z. Cao, Y.A. Wang, X. Peng, X. Wang, H.K. Sajja, L. Wang, H. Duan, C. Ni, C.A. Staley, W.C. Wood, X. Gao, S. Nie, Molecular imaging of pancreatic cancer in an animal model using targeted multifunctional nanoparticles, Gastroenterology 136 (2009) 1514–1525 e1512.

[92] J.H. Park, L. Gu, G. von Maltzahn, E. Ruoslahti, S.N. Bhatia, M.J. Sailor, Biodegradable luminescent porous silicon nanoparticles for in vivo applications, Nat. Mater. 8 (2009) 331–336.

[93] E. Pic, T. Pons, L. Bezdetnaya, A. Leroux, F. Guillemin, B. Dubertret, F. Marchal, Fluorescence imaging and whole-body biodistribution of near-infrared-emitting quantum dots after subcutaneous injection for regional lymph node mapping in mice, Mol. Imaging Biol. (2009) (Nov. 21, Electronic publication ahead of print), doi:10.1007/s11307-009-0288-y.

[94] T.S. Hauck, R.E. Anderson, H.C. Fischer, S. Newbigging, W. Chan, In vivo quantum-dot toxicity assessment, Small 6 (2010) 138–144.

[95] B. Ballou, B.C. Lagerholm, L.A. Ernst, M.P. Bruchez, A.S. Waggoner, Noninvasive imaging of quantum dots in mice, Bioconjug. Chem. 15 (2004) 79–86.

[96] M.L. Schipper, M. Iyer, A.L. Koh, Z. Cheng, Y. Ebenstein, A. Aharoni, S. Keren, L.A. Bentolila, J. Li, J. Rao, X. Chen, U. Banin, A.M. Wu, R. Sinclair, S. Weiss, S.S. Gambhir, Particle size, surface coating, and PEGylation influence the biodistribution of quantum dots in living mice, Small 5 (2009) 126–134.

[97] H. Maeda, J. Wu, T. Sawa, Y. Matsumura, K. Hori, Tumor vascular permeability and the EPR effect in macromolecular therapeutics: a review, J. Control. Release 65 (2000) 271–284.

[98] J.H. Kim, Y.S. Kim, K. Park, S. Lee, H.Y. Nam, K.H. Min, H.G. Jo, J.H. Park, K. Choi, S.Y. Jeong, R.W. Park, I.S. Kim, K. Kim, I.C. Kwon, Antitumor efficacy of cisplatin-loaded glycol chitosan nanoparticles in tumor-bearing mice, J. Control. Release 127 (2008) 41–49.

[99] K.H. Min, K. Park, Y.S. Kim, S.M. Bae, S. Lee, H.G. Jo, R.W. Park, I.S. Kim, S.Y. Jeong, K. Kim, I.C. Kwon, Hydrophobically modified glycol chitosan nanoparticles-encapsulated camptothecin enhance the drug stability and tumor targeting in cancer therapy, J. Control. Release 127 (2008) 208–218.

[100] G. Saravanakumar, K.H. Min, D.S. Min, A.Y. Kim, C.M. Lee, Y.W. Cho, S.C. Lee, K. Kim, S.Y. Jeong, K. Park, J.H. Park, I.C. Kwon, Hydrotropic oligomer-conjugated glycol chitosan as a carrier of paclitaxel: synthesis, characterization, and in vivo biodistribution, J. Control. Release 140 (2009) 210–217.

[101] K. Chen, J. Xie, H. Xu, D. Behera, M.H. Michalski, S. Biswal, A. Wang, X. Chen, Triblock copolymer coated iron oxide nanoparticle conjugate for tumor integrin targeting, Biomaterials 30 (2009) 6912–6919.

[102] H. Lee, K. Lee, I.K. Kim, T.G. Park, Synthesis, characterization, and in vivo diagnostic applications of hyaluronic acid immobilized gold nanoprobes, Biomaterials 29 (2008) 4709–4718.

[103] L. Yang, X.H. Peng, Y.A. Wang, X. Wang, Z. Cao, C. Ni, P. Karna, X. Zhang, W.C. Wood, X. Gao, S. Nie, H. Mao, Receptor-targeted nanoparticles for in vivo imaging of breast cancer, Clin. Cancer Res. 15 (2009) 4722–4732.

[104] Z. Medarova, L. Rashkovetsky, P. Pantazopoulos, A. Moore, Multiparametric monitoring of tumor response to chemotherapy by noninvasive imaging, Cancer Res. 69 (2009) 1182–1189.

[105] Z. Medarova, M. Kumar, S.W. Ng, A. Moore, Development and application of a dual-purpose nanoparticle platform for delivery and imaging of siRNA in tumors, Methods Mol. Biol. 555 (2009) 1–13.

[106] F. Duconge, T. Pons, C. Pestourie, L. Herin, B. Theze, K. Gombert, B. Mahler, F. Hinnen, B. Kuhnast, F. Dolle, B. Dubertret, B. Tavitian, Fluorine-18-labeled phospholipid quantum dot micelles for in vivo multimodal imaging from whole body to cellular scales, Bioconjug. Chem. 19 (2008) 1921–1926.